IV International Conference on Computational Methods for Coupled Problems in Science and Engineering
COUPLED PROBLEMS 2011
M. Papadrakakis, E. Oñate and B. Schrefler (Eds)

FREQUENCY PARAMETRIZATION TO NUMERICALLY PREDICT FLUTTER IN TURBOMACHINERY

M. Philit*, L. Blanc†, S. Aubert‡, W. Lolo†, P. Ferrand* and F. Thouverez†

*Laboratoire de Mécanique des Fluides et d'Acoustique (LMFA)
Université de Lyon, Ecole Centrale de Lyon; Université Lyon 1; INSA Lyon; CNRS UMR 5509
36, avenue Guy de Collongue, 69134 Ecully cedex, France
e-mail: mickael.philit@ec-lyon.fr, webpage: `http://lmfa.ec-lyon.fr`

†Laboratoire de Tribologie et de Dynamique des Systèmes (LTDS)
Ecole Centrale de Lyon; CNRS UMR 5513
36 avenue Guy de Collongue, 69134 Ecully cedex, France
e-mail: wilfried.lolo@ec-lyon.fr, webpage: `http://ltds.ec-lyon.fr`

‡ FLUOREM
Centre scientifique Auguste Moiroux
64 Chemin des Mouilles, 69134 Ecully Cedex, France
e-mail: stephane.aubert@fluorem.com, webpage: `http://www.fluorem.com`

Keywords: Fluid-Structure Coupling, Aeroelasticity, Turbine Blade Design, Flutter Margin Prediction, Meta-modeling

Abstract. In the quest for performance, modern turbomachinery designs are increasingly proner to flutter hazards. Unfortunately, their prediction is currently too expensive and inaccurate for industrial purpose. A significant step towards faster methods would consist in substituting a sequential algorithm to the classical iterative ones encountered in loose coupling strategies. The approach proposed here makes it possible through the use of a meta-model taking into account the sensitivity to design variables. This parametrized method is evaluated on a standard well referenced turbine configuration.

1 INTRODUCTION

Flutter is a critical issue presently facing the designers of turbomachinery blades. Indeed, modern turbomachinery configurations involve lighter and slender blades for efficiency. Meanwhile, the span tends to increase because of higher mass flow. Under these conditions, blade designs are more likely to react to the dynamic loading effects due to unsteady aerodynamics and conversely the flow itself is more likely to be affected by blade motion. In the worst case, a self-excited vibration can develop into resonance until the blade fails. These aeroelastic phenomena should of course be avoided and hence it is extremely important to be able to predict such unsteady aerodynamic interactions. Although experiments are of great importance in the understanding of these phenomena, they are sometimes hazardous. So, numerical simulation is the prefered mean to study flutter.

According to [1], two trends are significant in such simulation code structure. On the one hand, non-linear, fully integrated solvers have been developed for airfoil and wing and can be extended to turbomachinery blades. Fluid and structural domains are discretized together and the associated problems are solved simultaneously. Such tools are really complex and still require huge computer ressources. On the other hand, loosely coupled, linearized solvers allow for a faster simplified modelling. They are based on partially integrated solvers with alternate fluid and structure calculations synchronized more or less sophisticatedly depending on the way the data are transferred from one computation to the next via the fluid - structure interface [2, 3, 4]. The process is all the more CPU time-consuming as it is iterative.

The present paper is in line with the traditional approach of loose coupling. Indeed, the high stiffness of targeted blades allows to carry out fluid and structure computations in turn. But, instead of several iterations, the proposed approach is based on a single standard fluid computation followed by a structure computation *supplemented by high order derivatives* which provide information on the sensitivity of the fluid loading to variations of design parameters and operating conditions. The meta-model based on this parametrization is subjected to an optimization process which gives directly the characteristics of the coupled fluid-structure behavior without loop.

The paper outline is as follows. Firstly, theoretical issues are detailed: the proposed strategy is positionned with respect to classical approaches and the parametrization formalism is expressed in the specific case of a single parameter dependency. Secondly, the proposed methodology is supported by an application case to validate the flow parametrization and the ensuing meta-model.

2 A NEW LOOSE COUPLING STRATEGY

2.1 Fluid-structure behavior modelization

Structure and fluid calculations are carried out in turn to characterize the coupled system stability. They share geometric hypothesis. Bladed disks composed of identical sectors are considered. Thus cyclic symmetry properties are used to simulate one reference sector, including a single blade. The contribution of every sector is taken into account through periodic boundary conditions with phase lag, the so-called "Inter Blade Phase Angle" (IBPA).

First, the outline of the applied structure calculations is presented. No structural damping and no other excitation forces than the fluid loading induced by the considered blade displacement are assumed. A finite element discretization of the motion equation, written for the meshed reference sector, leads for a given IBPA value to:

$$\mathbf{M}\frac{d^2\mathbf{u}}{dt^2} + \mathbf{K}\mathbf{u} = \mathbf{f}, \tag{1}$$

where $\mathbf{u}$ is the vector of local structural displacements relative to equilibrium state under loading, $\mathbf{f}$ is the vector of aerodynamic forces, $\mathbf{M}$ and $\mathbf{K}$ are respectively mass and stiffness complex matrices (taking into account centrifugal effects if necessary). In the framework of linear stability analysis, the unknown $\mathbf{u}$ and the source term $\mathbf{f}$ are modeled as:

$$\mathbf{u} = A\mathbf{\Phi}e^{i\tilde{\omega}t}, \tag{2}$$

$$\mathbf{f} = A\mathbf{\Psi}e^{i\tilde{\omega}t} \tag{3}$$

where A is the displacement amplitude, $\mathbf{\Phi}$ and $\tilde{\omega}$ are the displacement mode shape and complex angular frequency, $\mathbf{\Psi}$ is the fluid modal loading. For a prescribed flow (i.e. $\mathbf{\Psi}$), Eq. 1 is then recasted as the following eigenvalue problem, the unknown being the mode ($\tilde{\omega}$, $\mathbf{\Phi}$):

$$(\mathbf{K} - \tilde{\omega}^2\mathbf{M})\mathbf{\Phi} = \mathbf{\Psi}(\tilde{\omega}, \mathbf{\Phi}). \tag{4}$$

It is to notice that, in general, this equation leads to complex eigenvalues :

$$\tilde{\omega} = \omega + i\alpha \;\; with \;\; \omega, \alpha \in \mathbb{R} \tag{5}$$

For stable configurations, ω is the damped natural angular frequency while α, positive, is the decay rate.

Next, the outline of the applied fluid calculations is presented. A viscous perfect gas subjected to turbulent flows is considered. A finite volume discretization of the Reynolds

Averaged Navier Stokes (RANS) equations supplemented with a turbulence model, written for the meshed fluid domain, leads to:

$$\frac{d}{dt}\left(\mathbf{J}(\mathbf{p})\ \mathbf{q}\right) + \mathbf{F}(\mathbf{p},\mathbf{q}) = \mathbf{0} \tag{6}$$

where $\mathbf{q}$ is the vector of nodal conservative and turbulent variables, $\mathbf{J}$ is the vector of mesh cells volume, $\mathbf{p}$ is the vector determining solid walls shape and boundary conditions, $\mathbf{F}$ is the non-linear function expressing the balance of convective and viscous fluxes. In the framework of linear stability analysis, the imposed instantaneous operating conditions $\mathbf{p}$ and the unknown $\mathbf{q}$ are modeled as :

$$\mathbf{p} = \overline{\mathbf{p}} + \delta\mathbf{p}e^{i\omega t}, \tag{7}$$

$$\mathbf{q} = \overline{\mathbf{q}} + \delta\mathbf{q}e^{i\omega t} \tag{8}$$

where ($\overline{\mathbf{p}}$, $\overline{\mathbf{q}}$) are the mean values and ($\delta\mathbf{p}$, $\delta\mathbf{q}$) are the small perturbation harmonic amplitudes at the prescribed angular frequency ω defined in Eq. 5. Then, the classical time-linearized Navier-Stokes approximation [5], where higher order terms are neglected, is applied. For a prescribed blade motion (i.e. $\overline{\mathbf{p}}$, $\delta\mathbf{p}$, ω), Eq. 6 is then recasted on the one hand as the Steady RANS equations (SRANS, Eq. 9) and on the other hand as the Linearized RANS equations (LRANS, Eq. 10), the unknown being ($\overline{\mathbf{q}}$, $\delta\mathbf{q}$) :

$$\mathbf{F}(\overline{\mathbf{q}},\overline{\mathbf{p}}) = \mathbf{0} \tag{9}$$

$$\left\{ i\omega\mathbf{J}(\overline{\mathbf{p}}) + \frac{\partial\mathbf{F}}{\partial\mathbf{q}}(\overline{\mathbf{q}},\overline{\mathbf{p}}) \right\}\delta\mathbf{q} = -\left\{ i\omega\overline{\mathbf{q}}\frac{\partial\mathbf{J}}{\partial\mathbf{p}}(\overline{\mathbf{p}}) + \frac{\partial\mathbf{F}}{\partial\mathbf{p}}(\overline{\mathbf{q}},\overline{\mathbf{p}}) \right\}\delta\mathbf{p} \tag{10}$$

Thus, fluid-structure coupling arises from the terms $\mathbf{\Psi}$ and $\delta\mathbf{p}$. Indeed, in Eq. 4, $\mathbf{\Psi}$ is a function of the unsteady fluid behavior and in Eq. 10, $\delta\mathbf{p}$ is a function of the unsteady wall displacement, namely:

$$\mathbf{\Psi} = \mathbf{\Psi}(\delta\mathbf{q}) \tag{11}$$

$$\delta\mathbf{p} = \delta\mathbf{p}(\tilde{\omega}, \mathbf{\Phi}) \tag{12}$$

Furthermore, $\tilde{\omega}$ is shared by Eqs. 4 and 10, but it is an output of Eq. 4 whereas its real part is an input of Eq. 10.

As a conclusion, to characterize the fluid-structure coupled system stability, the unknown to be calculated are ($\tilde{\omega}$, $\mathbf{\Phi}$, $\delta\mathbf{q}$) from Eqs. 4, 10, 11, 12. From these, the balance of mechanical energy exchanged between the fluid and the blade over one cycle will determine if the unsteady fluid loading is prone to amplify ($\alpha < 0$) or to damp ($\alpha > 0$) the blade oscillation.

2.2 Classical approaches

Modes calculation is often initialized in vacuum, i.e. $\mathbf{\Psi} = 0$. Let $(\tilde{\omega}_0, \mathbf{\Phi_0})$ be a solution of interest of Eq. 4 for such conditions. Usually, it is assumed that the mode shape $\mathbf{\Phi_0}$ remains unaffected by the flow : only the eigenfrequency $\tilde{\omega}$ is modified. As a result, the angular frequency shift, $\Delta\tilde{\omega} = \tilde{\omega} - \tilde{\omega}_0$, is sought instead of $\tilde{\omega}$ itself. $\Delta\tilde{\omega}$ is evaluated from the residual of Eq. 4 projected on the mode shape of interest $\mathbf{\Phi_0}$:

$$R(\Delta\tilde{\omega}) = \mathbf{\Phi_0}^H \left(\mathbf{K} - (\tilde{\omega}_0 + \Delta\tilde{\omega})^2\mathbf{M}\right) \mathbf{\Phi_0} - \mathbf{\Phi_0}^H \mathbf{\Psi}(\tilde{\omega}_0 + \Delta\tilde{\omega}, \mathbf{\Phi_0}). \tag{13}$$

where superscript ^{H} indicates the Hermitian conjugate. It is to notice that obviously, $R(0) \neq 0$ if $\mathbf{\Phi_0}$ and $\mathbf{\Psi}(\tilde{\omega}_0, \mathbf{\Phi_0})$ are not orthogonal. $\Delta\tilde{\omega}$ is sought such that it minimizes $R(\Delta\tilde{\omega})$, i.e. as the solution of:

$$\frac{\partial R^H R}{\partial \Delta\tilde{\omega}} = 0. \tag{14}$$

$\mathbf{\Psi}$ being an implicite intricate function of $\Delta\tilde{\omega}$, an iterative procedure is classically applied. $R(\Delta\tilde{\omega})$ is replaced by:

$$R^{(n)} = \mathbf{\Phi_0}^H \left(\mathbf{K} - (\tilde{\omega}_0 + \Delta\tilde{\omega}^{(n)})^2\mathbf{M}\right) \mathbf{\Phi_0} - \mathbf{\Phi_0}^H \mathbf{\Psi}(\tilde{\omega}_0 + \Delta\tilde{\omega}^{(n-1)}, \mathbf{\Phi_0}). \tag{15}$$

$\mathbf{\Psi}(\tilde{\omega}_0 + \Delta\tilde{\omega}^{(n-1)}, \mathbf{\Phi_0})$ is computed from Eqs. 11 and 10, using the previous iteration angular frequency $\tilde{\omega}^{(n-1)} = \tilde{\omega}_0 + \Delta\tilde{\omega}^{(n-1)}$. Then, $\Delta\tilde{\omega}^{(n)}$ is updated from Eq. 14 recasted as:

$$(\tilde{\omega}_0 + \Delta\tilde{\omega}^{(n)})\mathbf{\Phi_0}^H \mathbf{M} \mathbf{\Phi_0} R^{(n)} = 0 \tag{16}$$

Such a step from $\Delta\tilde{\omega}^{(n-1)}$ to $\Delta\tilde{\omega}^{(n)}$ is repeated as long as the projected fluid modal loading $\mathbf{\Phi_0}^H \mathbf{\Psi}$ changes significantly. The convergence of this procedure might be slow, or even hazardous, according to the dependence of $\mathbf{\Psi}$ on $\Delta\tilde{\omega}$.

2.3 Proposed parametrized sequential approach

The starting point of the proposed approach consists in modelizing the fluid modal loading by a truncated Taylor series expansion [6], as:

$$\mathbf{\Psi}(\tilde{\omega}_0 + \Delta\tilde{\omega}) \simeq \mathbf{\Psi}_0(\tilde{\omega}_0) + \frac{\partial \mathbf{\Psi}}{\partial \omega}(\tilde{\omega}_0)\Delta\tilde{\omega} + \frac{1}{2}\frac{\partial^2 \mathbf{\Psi}}{\partial \omega^2}(\tilde{\omega}_0)\Delta\tilde{\omega}^2 \tag{17}$$

Minimizing the residual $R(\Delta\tilde{\omega})$ reduces then in finding once the roots of the third order polynomial $\frac{\partial R^H R}{\partial \Delta\tilde{\omega}} = 0$ (Eq. 14), without further iterations. The novelty is in computing the derivatives of $\mathbf{\Psi}$ from those of $\delta\mathbf{q}$. Namely, deriving Eqs. 11 and 10 yields for first order terms:

$$\frac{\partial \mathbf{\Psi}}{\partial \omega}(\tilde{\omega}_0) = \frac{\partial \mathbf{\Psi}}{\partial \delta\mathbf{q}}(\delta\mathbf{q_0}) \ \frac{\partial \delta\mathbf{q}}{\partial \omega}(\tilde{\omega}_0) \tag{18}$$

with

$$\left\{ i\omega_0 \mathbf{J}(\overline{\mathbf{p}}) + \frac{\partial \mathbf{F}}{\partial \mathbf{q}}(\overline{\mathbf{q}}, \overline{\mathbf{p}}) \right\} \frac{\partial(\delta \mathbf{q})}{\partial \omega} = - \left\{ i\omega_0 \overline{\mathbf{q}} \frac{\partial \mathbf{J}}{\partial \mathbf{p}}(\overline{\mathbf{p}}) + \frac{\partial \mathbf{F}}{\partial \mathbf{p}}(\overline{\mathbf{q}}, \overline{\mathbf{p}}) \right\} \frac{\partial(\delta \mathbf{p})}{\partial \omega} - i \left\{ \mathbf{J}(\overline{\mathbf{p}}) \delta \mathbf{q_0} + \overline{\mathbf{q}} \frac{\partial \mathbf{J}}{\partial \mathbf{p}}(\overline{\mathbf{p}}) \delta \mathbf{p_0} \right\} \tag{19}$$

Recursive derivations yield then to higher order terms, such as $\frac{\partial^2 \mathbf{\Psi}}{\partial \omega^2}$. From the initial solution in vacuum ($\tilde{\omega}_0$, $\mathbf{\Phi_0}$), the proposed approach builds thus a parametrized meta-model of the flow unsteadiness comprising $\left(\delta \mathbf{q_0}, \frac{\partial \delta \mathbf{q}}{\partial \omega}, \frac{\partial^2 \delta \mathbf{q}}{\partial \omega^2}, ...\right)$, which leads to a meta-model of the fluid loading $\left(\mathbf{\Psi_0}, \frac{\partial \mathbf{\Psi}}{\partial \omega}, \frac{\partial^2 \mathbf{\Psi}}{\partial \omega^2}, ...\right)$. Using a Taylor series expansion, the residual $R(\Delta\tilde{\omega})$ (Eq. 13) is recasted as a polynomial in $\Delta\tilde{\omega}$, easily minimized. Iterations between structure and fluid calculations are therefore avoided. It is to notice that the left hand side matrices in Eqs. 10 and 19 are identical. So, $\left(\delta \mathbf{q_0}, \frac{\partial \delta \mathbf{q}}{\partial \omega}, \frac{\partial^2 \delta \mathbf{q}}{\partial \omega^2}, ...\right)$ are solutions of the same linear system with multiple RHS. Therefore, computational time can be significantly reduced by taking advantage of this feature.

2.4 Numerical methods

In the present paper, mechanical Eqs. 4 and 14 are solved with Ansys^{TM}tools and Matlab^{TM}. The steady flow solution (Eq. 6) is computed with Turbflow^{TM}solver [7, 8]. Eq. 10 is solved by the Fluorem's LRANS solver called Turb'Lin^{TM}, while Fluorem's Parametrized RANS(PRANS) solver called Turb'Sens^{TM}is used for Eq. 19.

The same numerical setup is shared by the three flow solvers. Fluid domain is discretized with multi-block structured meshes. Convective fluxes are evaluated with JST scheme [9] in which blade motion is taken into account through grid deformation (ALE formulation). Turbulence effects are modeled by Kok k-ω model [10], but turbulent variables are assumed constant during LRANS and PRANS computations following th classical "frozen turbulence" hypothesis. To solve the linear systems, a GMRES Krylov algorithm is used instead of a more usual time marching algorithm as it is proven to be more stable and robust [11].

The partial derivatives in Eqs. 10 and 19 are exactly computed by a set of functions generated by Fluorem "in house" Automatic Derivation (AD) Tool, applied to the core **F** function (Eq. 6) of Turb'Flow. This tool was originally intended to parametrize steady flow solutions [12, 13].

3 VALIDATION ON A TURBINE CONFIGURATION

3.1 Test case overview

A cascade aeroelastic configuration is chosen so that it provides realistic flow boundary conditions and can exhibit flutter properties. It is a well referenced subsonic turbine configuration (Standard Configuration number 4 in [14]).

Results of the measurements are reported for four different IBPAs (270°, 180°, 90° and 0°) by Bölcs and Fransson [14]. The experimental apparatus involves a highly loaded annular cascade of blades that are bending in a controled oscillatory manner.The frequency of the oscillation remains nearly constant as well as the amplitude. Investigations have been performed for the first bending mode at a constant exit Mach number of 0.9. The experimental reduced frequency is then $k = 0.107$. The full finite element model and the single sector simulated are presented on Fig. 1. Fig. 2 presents the steady Mach number distribution obtained when solving Eq. 6.

The local response of the flow is quantified through the complex pressure coefficient defined for a surface element ($\mathbf{n}dS$) of the blade, as:

$$\widetilde{c}_p = \frac{\mathbf{\Psi}(\Delta\tilde{\omega}).\mathbf{n}}{dS(P_t - P_s)} \tag{20}$$

where $P_t - P_s$ is the dynamic pressure taken upstream.

The global energy exchange between the blade and the flow is resolved according to Fransson [14]. The unsteady aerodynamic work coefficient is integrated over the entire blade for a cycle of oscillation yielding to the aerodynamic damping coefficient :

$$\Xi = \frac{-1}{(P_t - P_s)} \Im(\mathbf{\Phi_0}^H \mathbf{\Psi}(\Delta\tilde{\omega})) \tag{21}$$

By definition, if the coefficient is negative, the forcing of the blade adds energy making the system unstable. Thus, this coefficient will be evaluated for illustrative purpose.

3.2 Coupling validation

Herein, the new methodology is demonstrated for an IBPA of 0 degree with regards to the frequency parameter. Mode shape, IBPA and operating conditions are held fixed. According to experimental data, IBPA 0 case is near the stability frontier.

Following Eq. 4, a modal analysis in vacuum provides the first bending mode shown in Fig. 1. Modal frequency is computed at $149.91\,Hz$. The result is consistent with experimental data.

Fig. 3 shows the unsteady pressure coefficient defined in Eq. 20, represented through its module and phase in degrees over the blade as well as its derivatives with respect to angular frequency (computed with Eqs. 10 and 19).

In order to investigate the validity of Eq. 17 approximation, three characteristic locations on the blade are chosen as illustration. Numerical probes are thus picked out at the leading edge , and on the pressure and suction sides (green, red and blue points displayed in Fig 2 respectively). These three points have been chosen because of their different sensitivity to the steady aerodynamic flow (Fig. 3). On the Fig. 4, the $\widetilde{c}_p$ module behaves almost as a parabolic curve and the phase is non-linear. At leading edge the module and phase depend quasi-linearly on the frequency as shown in Fig. 4. On the pressure side, the phase has a parabolic profile.

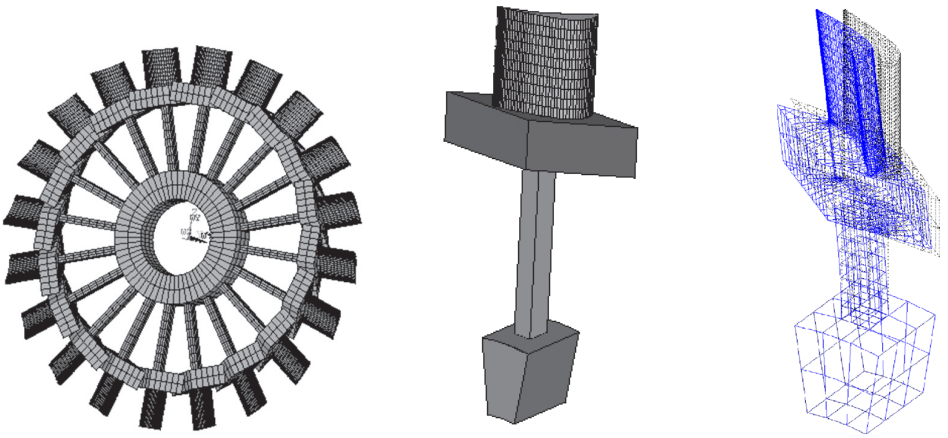

Figure 1: Model of the bladed disk: complete model (left) , reference sector (middle), targeted mode shape (right)

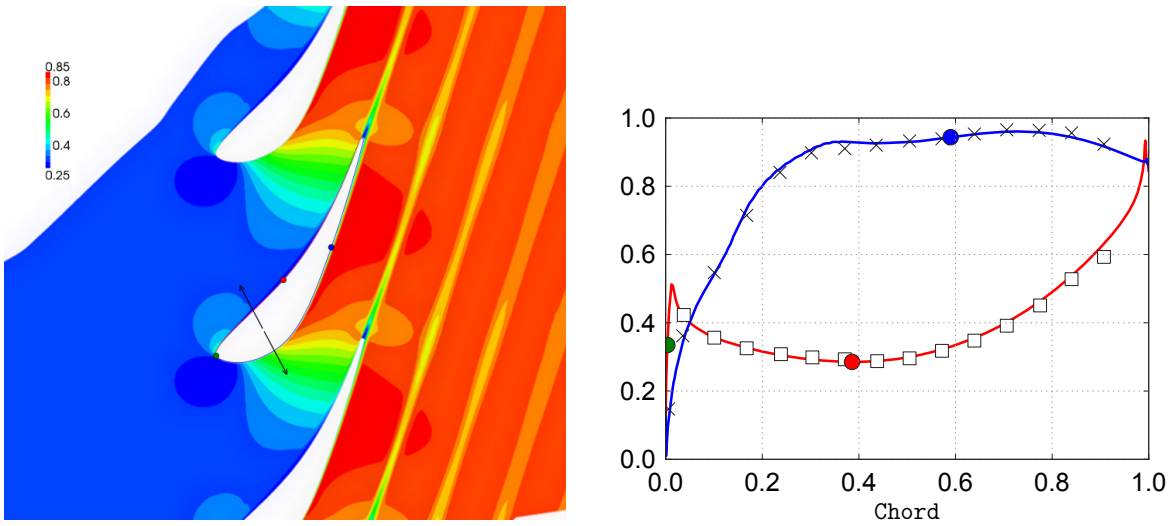

Figure 2: Mach number in blade-to-blade view

Overall, the approximant is well suited. At each position on the blade, the different approximations (lines) are obtain by extrapolating $\widetilde{c}_p$ from Eqs. 20 and 17. They agree very well with direct computation of $\widetilde{c}_p$ (symbols) using only Eq. 10, and particularly on the phase component. This is promising because the stability analysis is highly related to the phase status. From a local aerodynamic point of view, the model behaves well, it is thus expected to do as well from a global point of view.

As the result of this parametric study, the damping coefficient (Eq. 21) versus the oscillation frequency is presented in Fig. 5. The first order model takes only into account the first derivative of loadings giving a rough idea on the linear local (in terms of angular

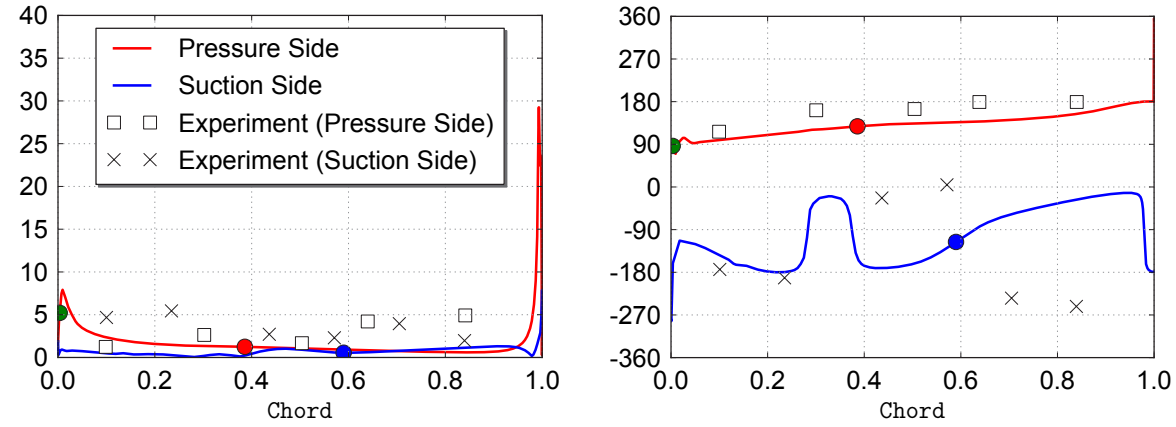

(a) zero order term $\widetilde{c}_{p0}$

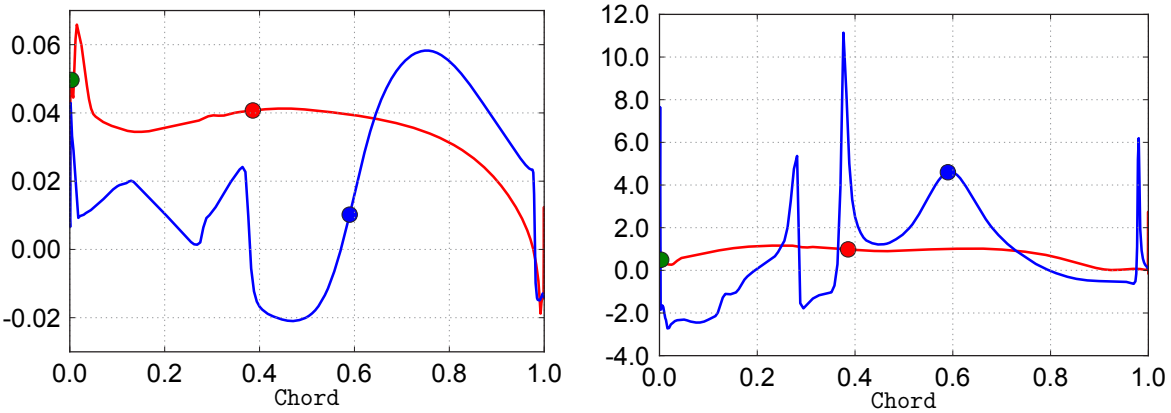

(b) first order derivative $\partial\widetilde{c}_p/\partial\omega$

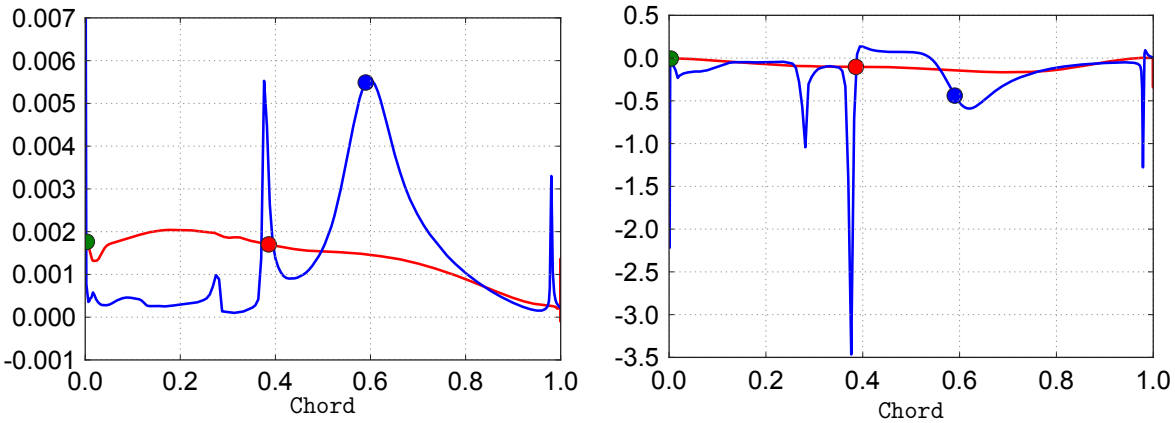

(c) second order derivative $\partial^2\widetilde{c}_p/\partial\omega^2$

Figure 3: Amplitude (left) and phase (right) of the pressure coefficient and its derivatives

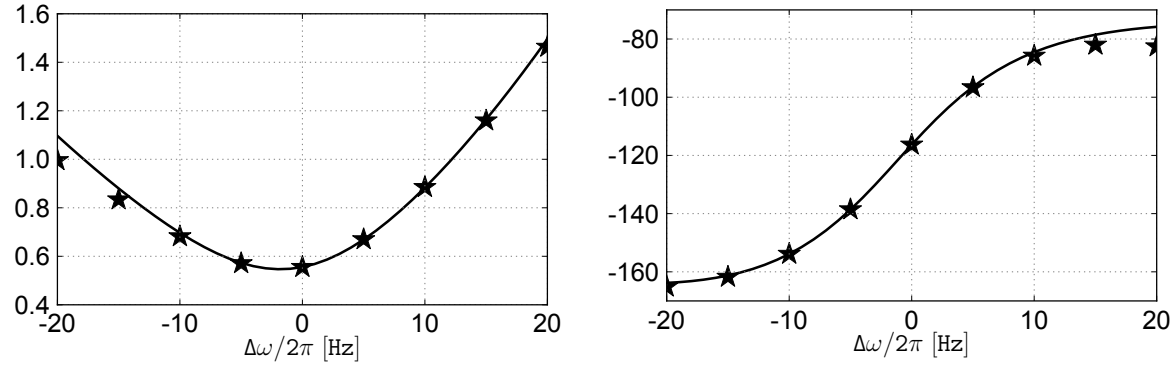

(a) Suction Side (blue)

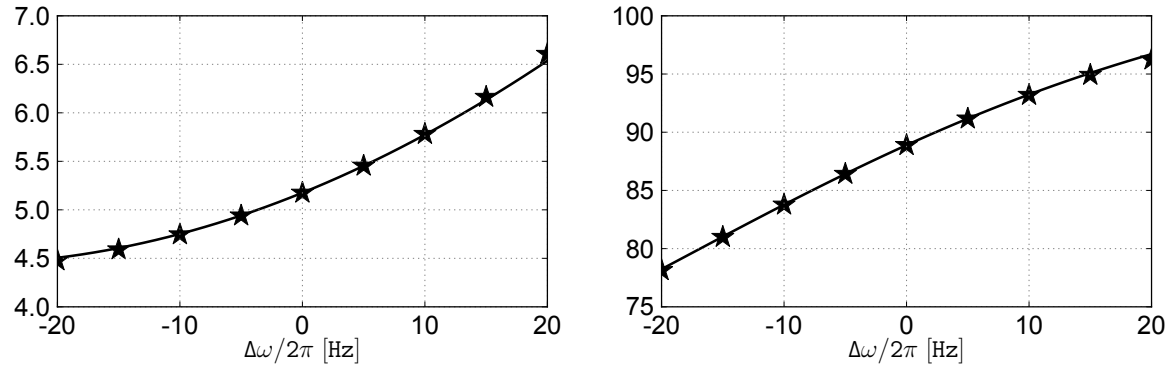

(b) Leading Edge (green)

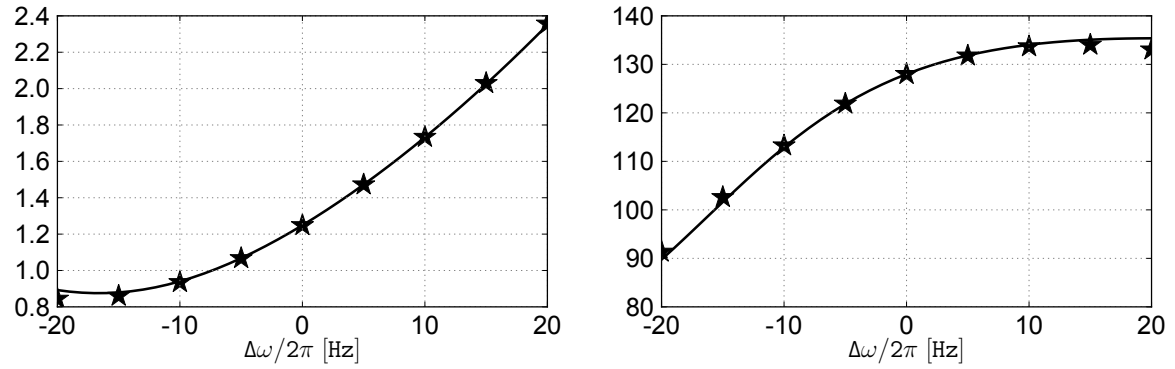

(c) Pressure Side (red)

Figure 4: Comparison at numerical probes of pressure coefficient amplitude (left) and phase (right)

frequency) behavior of the flow. Finally the second order model brings a good agreement with direct computations by adding the effect of second order derivatives. In this case, one could notice that with the second order global damping coefficient approximation the system is predicted marginaly stable when angular frequency is reduced. On the contrary,

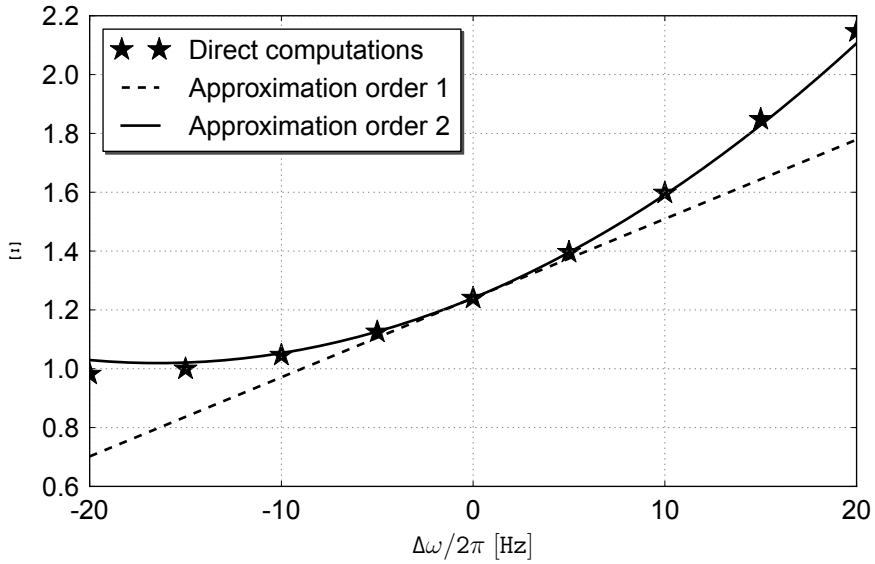

Figure 5: Aerodynamic damping sensitivity to frequency

IBPA	freq. in vacuum (Hz)	freq. in flow (Hz)	relative variation (%)	Ξ
0°	149.91	149.87	−0.03	1.24
90°	149.88	150.20	0.21	8.40
180°	149.85	150.58	0.49	6.03
270°	149.88	150.31	0.28	−0.77

Table 1: Frequency shifts and aerodynamic damping coefficient for different values of IBPA

with first order only, it turns to be unstable.

Because residue R's minimization (see Eq. 13) gives the frequency shifts, a special attention is paid to the validation of its estimation. Thus, the evolution of $R^H R$ according to frequency is drawn on Fig. 6 for different IBPA values: a comparison is performed between functions obtained through Eq. 17 and computed points using Eq. 15. The agreement is very satisfactory: the minima are found at the same frequencies for both methods whatever the considered IBPA. Moreover the approximate residues fit the reference values in a wide frequency range, around ±10% of the frequency estimated in vacuum.

The frequency shifts associated with the minima are gathered in tab. 1. These shifts are relatively small, revealing quite a weak influence of the fluid on the frequency. Larger variations would be expected with a lower stiffness of the structure, but this has to be tested numerically.

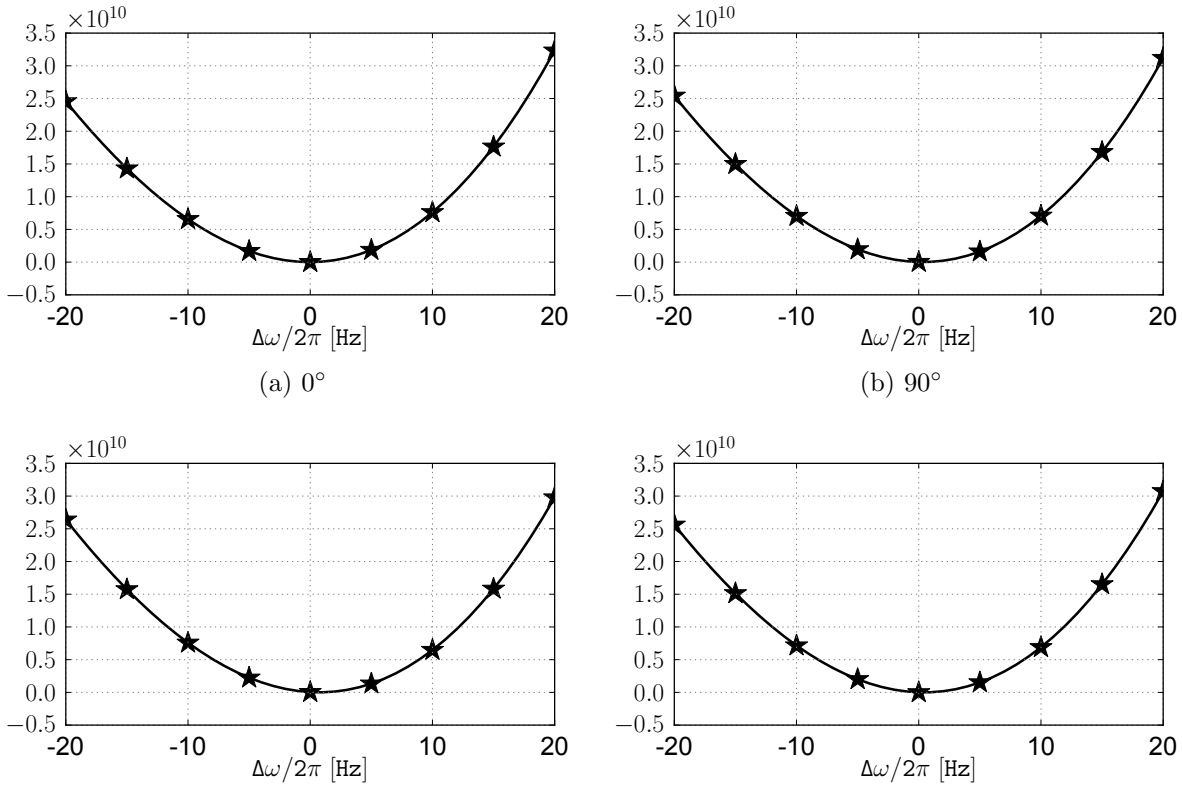

(a) 0° (b) 90°

(c) 180° (d) 270°

Figure 6: $R^H R$ evolution for different IBPA values

4 CONCLUSIONS

The feasibility of a non-iterative fluid-structure loose coupling approach dedicated to turbomachinery flutter problematics has been demonstrated. The new strategy is based on a parametrization that is made possible thanks to an "in-house" Automatic Derivation Tool that provides the aerodynamic force gradients with respect to angular frequency. The flow influence on mode's eigenfrequency has been investigated to provide, in a time-saving way, the characteristics of the mode. However, any design variable affecting stability margin could have been chosen, such as variations stemming from either structural response (implying mode shape or IBPA) or from operating conditions (rotating velocity, Mach number, flow incidence).

The gain of CPU time obtained by avoiding the burden of iterating inside the fluid-structure coupling procedure lets foresee applications of this approach in other domains where loose coupling is used, such as forced response computation, with or without mistuning calculation. The formalism could also be useful in presence of structural non-linearities.

ACKNOWLEDGEMENTS

- The authors, who are members of the french ANR project ANR-08-2009 CapCAO (standing for "parametrization-aided optimized aeroelastic design"), wish to thank ANR (Agence National de la Recherche) for its generous sponsoring.
- CINES (Centre Informatique National de l'Enseignement Supérieur), which provides the computational support of the present work, is also gratefully acknowledged.
- The authors would like to especially thank Vsevolod Kharyton and Jean-Pierre Laîné for their helpful contributions.

REFERENCES

[1] Marshall, J. G. & Imregun, M. Review of aeroelasticity methods with emphasis on turbomachinery applications. *Journal of Fluids and Structures* **10**, 237–267 (1996).

[2] He, Z., Epureanu, B. I. & Pierre, C. Parametric study of the aeroelastic response of mistuned bladed disks. *Computers and Structures* **85**, 852–865 (2007).

[3] Tran, D. M. Multi-parameter aerodynamic modeling for aeroleastic coupling in turbomachinery. *Journal of Fluids and Structures* **25**, 519–534 (2009).

[4] Tran, D. M., Liauzun, C. & Labaste, C. Methods of fluid-structure coupling in frequency and time domains using linearized aerodynamics for turbomachinery. *Journal of Fluids and Structures* **17**, 519–534 (2003).

[5] Holmes, D. G., Mitchell, B. E. & Lorence, C. B. Three dimensional linearized Navier-Stokes calculations for flutter and forced response. In *Proceedings of the 8th International Symposium of Unstead Aerodynamics and Aeroelasticity of Turbomachines*, 211–224 (1997).

[6] Karpel, M. Design for active and passive flutter suppression and gust alleviation. *NASA CR3482* (1981).

[7] Smati, L., Aubert, S., Ferrand, P. & Massao, F. Comparison of numerical schemes to investigate blade flutter. In *Proceedings of the 8th International Symposium of Unstead Aerodynamics and Aeroelasticity of Turbomachines* (1997).

[8] Smati, L., Aubert, S. & Ferrand, P. Numerical study of unsteady shock motion to understand transonic flutter. In *Proceedings of Euromech 349 on Simulation of fluid-structure interaction in aeronautics* (1996).

[9] Jameson, A., Schmidt, W. & Turkel, E. Numerical solutions of the Euler equations by finite volume methods with Runge-Kutta time stepping schemes. *AIAA paper 81-1259* (1981).

[10] Kok, J. Resolving the dependence on free-stream value for k-ω turbulence model. *AIAA Journal* **38**, 1292–1295 (2000).

[11] Chassaing, J.-C., Gerolymos, G. A. & Jérémiasz, J.-G. GMRES solution of compressible linearized Navier-Stokes equations without pseudo-time-marching. In *44th AIAA Aerospace Sciences Meeting* (2006).

[12] Aubert, S. *et al.* Optimisation of a gas mixer using a new parametric flow solver. In *ECCOMAS Computational Fluid Dynamics Conference*, 17 (2001).

[13] Moreau, S. *et al.* Parametric study of a fan blade cascade using a new parametric flow solver Turb'Opty. In *ASME Joint US-European Fluids Engineering Conference*, 10 (Montreal, Canada, 2002).

[14] Bölcs, A. & Fransson, T. Aeroelasticity in turbomachines. Comparison of theoretical and experimental cascade results. *Communication du laboratoire de thermique appliquée et de turbomachines de l'EPFL* **13** (1986).